

The Reaction of Singlet Oxygen with Enecarbamates: A Mechanistic Playground for Investigating Chemoselectivity, Stereoselectivity, and Vibratioselectivity of Photooxidations

J. SIVAGURU,^{*,†} MARISSA R. SOLOMON,[‡] THOMAS POON,[§]
 STEFFEN JOCKUSCH,[‡] SARA G. BOSIO,[‡] WALDEMAR ADAM,^{*,‡,||}
 AND NICHOLAS J. TURRO^{*,‡}

[†]The Department of Chemistry and Molecular Biology, North Dakota State University, Fargo, North Dakota 58105, [‡]The Department of Chemistry, Columbia University, New York, New York 10027, [§]Joint Science Department, W.M. Keck Science Center, 925 North Mills Avenue, Claremont McKenna, Pitzer, and Scripps Colleges, Claremont, California 91711, [‡]Institute für Organische Chemie, Universität Würzburg, D-97074 Würzburg, Germany, ^{||}The Department of Chemistry, University of Puerto Rico, Facundo Bueso 110, Rio Piedras, Puerto Rico 00931

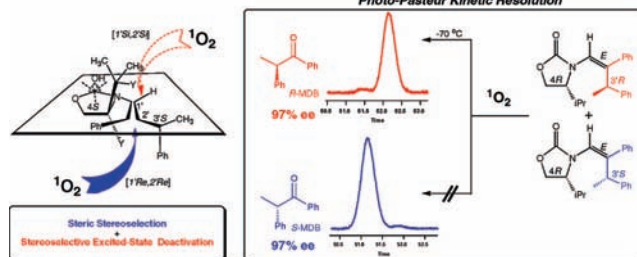
RECEIVED ON MAY 21, 2007

CONSPECTUS

Photochirogenesis, the control of chirality in photoreactions, is one of the most challenging problems in stereocontrolled photochemistry, in which the stereodifferentiation has to be imprinted within the short lifetime of the electronically excited state. Singlet oxygen ($^1\text{O}_2$), an electronically excited molecule that is known to be sensitive to vibrational deactivation, has been selected as a model case for testing stereoselective control by vibrational deactivation. The stereoselectivity in the reaction of $^1\text{O}_2$ with *E/Z* enecarbamates **1**, equipped with the oxazolidinone chiral auxiliary, has been examined for the mode selectivity ($[2 + 2]$ -cycloaddition versus *ene*-reaction) and the stereoselectivity in the oxidative cleavage of the alkenyl functionality to the methyldeoxybenzoin (MDB) product. Through the appropriate choice of substituents in the enecarbamate, the mode selectivity (*ene* versus $[2 + 2]$), which depends on the alkene geometry (*E* or *Z*), the steric bulk of the oxazolidinone substituent at the C-4 position, and the C-3' configuration on the side chain, may be manipulated. Phenethyl substitution gives exclusively the $[2 + 2]$ -cycloaddition product, irrespective of the alkene geometry. The stereoselection in the resulting methyldeoxybenzoin (MDB) product is examined in a variety of solvents as a function of temperature by using chiral GC analysis. The extent (% ee) as well as the sense (*R* versus *S*) of the stereoselectivity in the MDB formation for the *E* isomer depends significantly on solvent and temperature, whereas the corresponding *Z* isomers are not affected by such variations. The complex temperature and solvent effects are scrutinized in terms of the differential activation parameters ($\Delta\Delta S^\ddagger$, $\Delta\Delta H^\ddagger$) for the photooxygenation of *E/Z*-enecarbamates in various solvents at different temperatures. The enthalpy–entropy compensations provide a mechanistic understanding of the temperature dependence of the ee values for the MDB product and the difference in the behavior between the *Z* and *E* enecarbamates. The *E* enecarbamates show a relatively high contribution from the entropy term and an appreciable contribution from the enthalpy term; both terms possess the same sign. In contrast, the corresponding relative insensitivity of *Z* enecarbamates to temperature and solvent variation is convincingly explained by the near-zero $\Delta\Delta S^\ddagger$ and $\Delta\Delta H^\ddagger$. Such effects, associated with temperature- and solvent-dependent conformational factors, are most likely dictated by the stereogenic center at the C-3' phenethyl substituent.

The high stereocontrol during the photooxygenation of the chiral enecarbamates is shown to be independent of the steric demand of the oxazolidinone substituent at the C-4 position. In view of the reduced stereocontrol on deuteration of the oxazolidinone substituent at the C-4 position, we propose that the *unusual stereoselective vibrational quenching* of the attacking singlet oxygen (excited-state reactivity), a novel mechanistic concept, works in concert with the *usual steric impositions* (ground-state reactivity) exercised by the substituents to afford the high stereoselectivity observed in the dioxetane product during the $[2 + 2]$ cycloaddition. Such synergistic interplay is held responsible for the highly stereoselective photooxidative cleavage of the chiral enecarbamates. The efficacy of stereocontrol in this photooxidation is demonstrated by kinetically resolving the epimers of the enecarbamate cleavage product (MDB) in essentially perfect stereoselectivity, a new methodology that we coin “photo-Pasteur-type kinetic resolution”.

conspectus:



1. Introduction

The control of stereoselectivity in photoreactions is a formidable challenge.^{1–3} Electronically excited states are generally short-lived and possess a negligible activation barrier for photophysical deactivation, which imposes a “clock” on reaction selectivity: if a reaction cannot achieve the desired stereocontrolled pathway within the short lifetime of an electronically excited state, it can usually take another photophysical trajectory to reach the ground state.⁴ Classical stereoselectivity in ground-state reactions is often controlled by steric effects, which create energetically different diastereomeric relationships along reaction trajectories. But due to the negligible activation barrier, photoreactions may not be controlled solely on steric grounds. In this Account, we speculate whether in photoreactions, the stereoselectivity may be determined by controlling the lifetimes of excited states along different diastereomeric pathways; such speculation suggested to us the possibility of a novel “deactivation control” of stereoselectivity in photoreactions. A candidate for exhibiting deactivation control of stereoselectivity is singlet molecular oxygen (¹O₂), an electronically excited state that is known to be very sensitive to vibrational deactivation (¹O₂ is deactivated ~10 times faster by C–H vibrations than by C–D vibrations).^{5–7} Of course, classical steric hindrance may, however, offset vibrational selectivity, but in view of the small size of ¹O₂, steric effects should be relatively ineffective in controlling the stereoselectivity of photooxygenations. Thus, we selected ¹O₂ as a candidate for testing the conjecture that the reaction stereochemistry of an electronically excited state may be controlled by selective deactivation of one stereochemical pathway.

Oxazolidinone-functionalized enecarbamates^{8–10} **1** (Chart 1) were chosen as substrates for the reaction with ¹O₂ because these substrates may be readily manipulated to provide a wide scope of systematic stereochemical variations (highlighted by a specific example, namely, the 4*S*/3'*R* diastereomer of the *Z*-**1i** enecarbamate in Chart 1) to examine the stereochemical course of photooxygenation through (i) the *R/S* configuration of the C-4 position in the oxazolidinone chiral auxiliary, (ii) the *E/Z* geometry of the alkene (the reaction center), and (iii) the *R/S*-configuration at the C-3' position in the R² and R³ substituents.

In addition to stereochemistry, the chemoselectivity of the competing [2 + 2]-cycloaddition and *ene* reaction may be investigated.⁸ The stereochemistry of the [2 + 2]-cycloaddition reaction of **1** with ¹O₂ may be substantially

influenced by a proper choice of the size and configuration at the C-4 oxazolidinone substituent, the *E/Z*-alkene geometry, and the configuration at the C-3' position, to enable a high measure of variation through directing conformational factors that may be affected considerably by solvent and temperature.^{8,11–13}

2. Mode Selectivity (Chemoselectivity) of the ¹O₂ Reaction with Enecarbamates

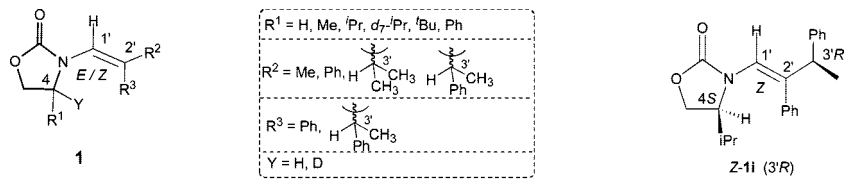
The *Z*- and *E*-enecarbamates **1** possess *ene*-active allylic hydrogen atoms at the R² and R³ substituents, namely, the methyl (Chart 1, entries 1–10), the isopropyl (Chart 1, entries, 11), and the phenethyl (Chart 1, entries 12–21) groups, for which both [2 + 2]-cycloaddition and *ene*-reaction are possible (Scheme 1). Indeed, the *Z* enecarbamates favor the [2 + 2]-cycloaddition product **2**, whereas the corresponding *E*-isomers prefer the *ene*-product **3**; however, the phenethyl-substituent (Table 1, entries 12–19) gives *exclusively* the [2 + 2]-cycloadduct **2**, irrespective of the alkene geometry (Table 1).

This *Z/E*-dependent dichotomy in mode selectivity may be understood in terms of the established⁸ orbital-directing effect between the HOMO of the enecarbamate (vinyllic nitrogen) and the LUMO of the incoming ¹O₂, which directs the attack onto the side that bears the nitrogen atom (Scheme 2, top).⁸ In the case of the reaction of ¹O₂ with *E/Z*-enecarbamates **1g–k** with phenethyl substituents, only dioxetane is formed in an outstanding selectivity of >99:1, which indicates the dominance of the [2 + 2] mode over the *ene* reaction (Table 1, entries 12–19). This very high selectivity is due to two factors, namely, the directing effect of the vinyllic nitrogen atom that favors [2 + 2]-cycloaddition, and the 1,2-allylic strain that disfavors the competing *ene* reaction (Scheme 2, bottom).⁸ In the preferred conformer of the enecarbamates with phenethyl (*Z*-**1g–k**) or isopropyl (*Z*-**1f**) substitution, the allylic hydrogen atom to be abstracted cannot assume a coplanar alignment with the π orbital of the alkene because of steric repulsion between the methyl group at the C-3' position and the vinyllic phenyl substituent (Scheme 2, bottom).⁸

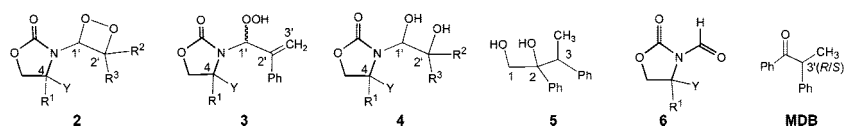
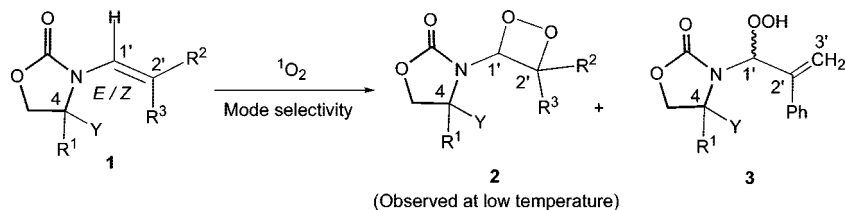
3. Stereoselectivity in the Competing [2 + 2] and *Ene* Reactions

As mentioned above, three stereochemical features (the stereogenic centers at the C-4 position, the C-3' position, and the *Z/E* geometry) make these enecarbamates information-rich substrates for investigating photooxygenation leading to dioxetanes **2** and *ene*-products **3** (Scheme 1). The stereochemical

CHART 1. Structure Matrix



Entry	Substrates	R ¹	R ²	R ³	Y
1	Z-1a	H	Me	Ph	H
2	E-1a	H	Ph	Me	H
3	Z-1b	Me	Me	Ph	H
4	E-1b	Me	Ph	Me	H
5	Z-1c	ⁱ Pr	Me	Ph	H
6	E-1c	ⁱ Pr	Ph	Me	H
7	Z-1d	^t Bu	Me	Ph	H
8	E-1d	^t Bu	Ph	Me	H
9	Z-1e	Ph	Me	Ph	H
10	E-1e	Ph	Ph	Me	H
11	Z-1f	ⁱ Pr	ⁱ Pr	Ph	H
C-3' Phenethyl-substitution					
12	Z-1g	H	Ph(Me)CH	Ph	H
13	Z-1h	Me	Ph(Me)CH	Ph	H
14	E-1h	Me	Ph	Ph(Me)CH	H
15	Z-1i	ⁱ Pr	Ph(Me)CH	Ph	H
16	<i>d</i> ₈ -Z-1i	<i>d</i> ₇ - ⁱ Pr	Ph(Me)CH	Ph	D
17	E-1i	ⁱ Pr	Ph	Ph(Me)CH	H
18	<i>d</i> ₈ -E-1i	<i>d</i> ₇ - ⁱ Pr	Ph	Ph(Me)CH	D
19	Z-1j	^t Bu	Ph(Me)CH	Ph	H
20	E-1j	^t Bu	Ph	Ph(Me)CH	H
21	Z-1k	Ph	Ph(Me)CH	Ph	H

SCHEME 1. Mode Selectivity ([2 + 2] Cycloaddition versus Ene Reaction) in the Photooxygenation of Oxazolidinone-Functionalized *E/Z* Enecarbamates **1**

complexity of the [2 + 2] versus the *ene* reaction is exhibited in Figure 1. As exemplars, consider the two possible diastereomeric [2 + 2]-dioxetanes 1'*S*,2'*S*-**2c** and 1'*R*,2'*R*-**2c** and the two possible diastereomeric *ene*-hydroperoxides *ul*-**3c** and *lk*-**3c** (Figure 1, R¹ = isopropyl), derived from the photooxygenation of the enecarbamate Z-**1c**. First, the diastereoselec-

tivity for the *ene*-product **3** shall be considered; subsequently, the selectivity of the more complex dioxetanes **2** shall be elaborated.

3.1. The Stereoselectivity in the Ene Reaction of ¹O₂ with Enecarbamates. The pertinent diastereoselectivity data of the *ene*-product **3**, obtained in the photooxygenation of

TABLE 1. Mode Selectivity and Diastereoselectivity in the Photooxygenation^{a,b} of Oxazolidinone-Functionalized Enecarbamates **1**

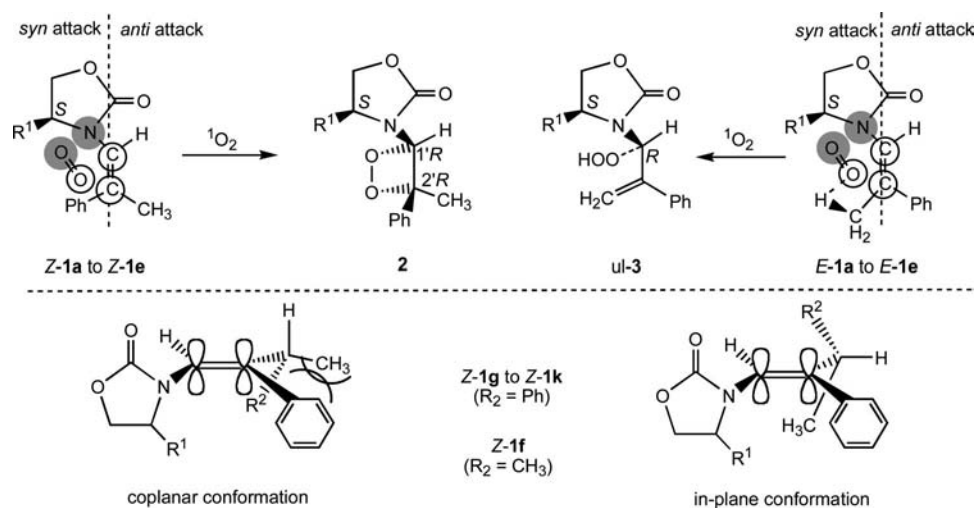
entry	substrates	configuration		mode, [2 + 2]/ene, 2/3	diastereomeric ratio (dr)	
		C-4	C-3'		3 ul/lk	2 (1'S,2'S)/(1'R,2'R)
1	Z-1a			80:20		
2	E-1a			15:85		
3	Z-1b	(<i>R</i>)-Me		80:20	53:47	>98:2
4	E-1b	(<i>R</i>)-Me		16:84	88:12	<i>f</i>
5	Z-1c	(<i>R</i>)- ^{<i>i</i>} Pr		75:25	56:44	99:1
6	E-1c	(<i>R</i>)- ^{<i>i</i>} Pr		36:64	83:17	<i>f</i>
7	Z-1d	(<i>S</i>)- ^{<i>t</i>} Bu		60:19 ^d	95:5	1:99
8	E-1d	(<i>S</i>)- ^{<i>t</i>} Bu		23:77	91:9	<i>f</i>
9	Z-1e	(<i>S</i>)-Ph		87:13	85:15	1:99
10	E-1e	(<i>S</i>)-Ph		8:92	71:29	<i>f</i>
11	Z-1f	(<i>R</i>)- ^{<i>i</i>} Pr		>99:1		98:2
12	Z-1g		(<i>R/S</i>)-Ph(Me)CH	>99:1	<i>c</i>	50:50
13	Z-1h	(<i>R</i>)-Me	(<i>S</i>)-Ph(Me)CH	>99:1	<i>c</i>	99:1
14	Z-1i	(<i>R</i>)- ^{<i>i</i>} Pr	(<i>S</i>)-Ph(Me)CH	>99:1	<i>c</i>	99:1
15 ^e	Z-1i	(<i>S</i>)- ^{<i>i</i>} Pr	(<i>S</i>)-Ph(Me)CH	>99:1	<i>c</i>	1:99
16 ^e	<i>d</i> ₈ - Z-1i	<i>d</i> ₇ -(<i>S</i>)- ^{<i>i</i>} Pr	(<i>S</i>)-Ph(Me)CH	>99:1	<i>c</i>	10:90
17		(<i>S</i>)- ^{<i>t</i>} Bu	(<i>R</i>)-Ph(Me)CH	>99:1	<i>c</i>	1:99
18	Z-1k	(<i>S</i>)-Ph	(<i>S</i>)-Ph(Me)CH	>99:1	<i>c</i>	1:99
19 ^e	E-1i	(<i>R</i>)- ^{<i>i</i>} Pr	(<i>S</i>)-Ph(Me)CH	>99:1	<i>c</i>	99:1 ^g

^a Photooxygenations run in CDCl₃ at -32 °C. TPFPP tetrakis(pentafluorophenyl)porphine as sensitizer until complete conversion of the enecarbamate **1**.

^b Determined by ¹H-NMR spectroscopy (error ± 5% of the stated value); mass balance >95% for all reactions. ^c In entries 12–19, the *ene* product corresponding to **3** was not observed. ^d 21% of the endoperoxide was obtained corresponding to ¹O₂ addition to both the alkene double bond and the phenyl ring (R₃: Ph).

^e CD₂Cl₂ was used as solvent. ^f Not determined. ^g (1'S,2'R)/(1'R,2'S) ratio.

SCHEME 2. Orbital control in the mode selectivity [(2 + 2) cycloaddition (top left) to form a dioxetane and *ene* reaction to form a hydroperoxide (top right)] for ¹O₂ attack from below the paper plane on the *Z*- and *E*-configured enecarbamates **1a–e** and the sterically hindered, unpreferred coplanar (bottom left) and the less sterically hindered, preferred in-plane (bottom right) conformations of the abstractable allylic hydrogen atom in the *Z*-configured enecarbamates **1f–k**



both *Z/E*-enecarbamates **1**, are summarized in Table 1. The major diastereomer has the *unlike* (*ul*) configuration (Figure 1) in both cases. The stereoselectivity of the *Z* substrate varies over a wider range [from 53:47 (entry 3) to 95:5 (entry 9)] and is subject to more effective stereocontrol than that of the *E* isomer [from 71:29 (entry 10) to 91:9 (entry 8)]; no diastereomers are possible for *E*-**1b** (R¹ = H, entry 2). Mechanistically (Scheme 2), these stereochemical results reflect the steric demand of the R¹ substituent at the C-4 position. Clearly, the

sterically controlled diastereofacial differentiation in the *ene* reactivity of **1** is more pronounced for the *Z* than the *E* isomers.

3.2. The Stereoselectivity of the [2 + 2]-Cycloaddition of ¹O₂ with the Enecarbamates. The absolute configuration of the dioxetane **2** upon [2 + 2]-cycloaddition of ¹O₂ with *Z*-**1** was established by chemical correlation,⁸ namely by the conversion of **2** to its diol **5** (Scheme 3). From these correlations, it was found that the [2 + 2]-cycloaddition proceeds

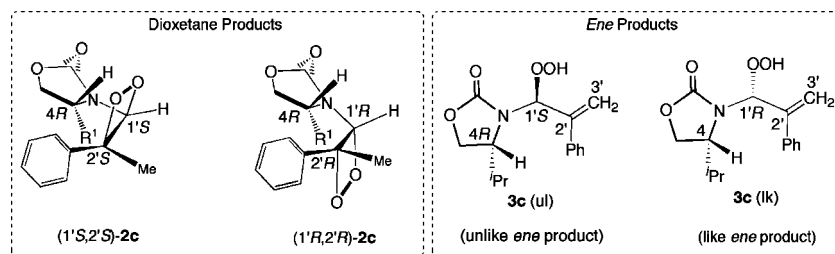
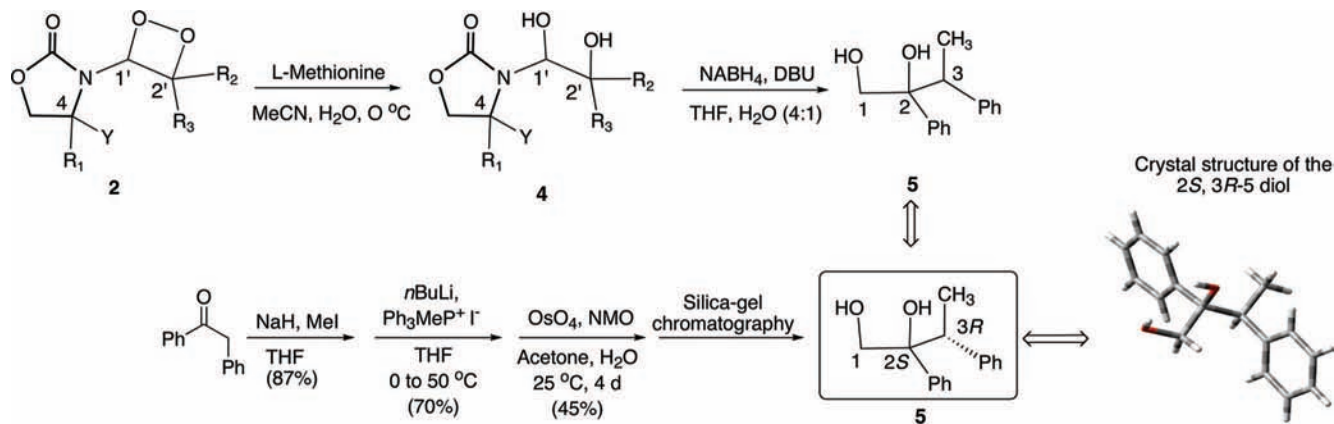
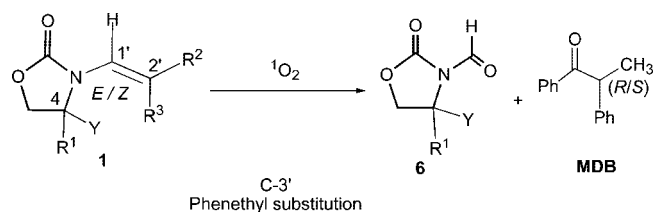


FIGURE 1. Representative diastereomers of the dioxetanes $1'S,2'S$ -**2c**, $1'R,2'R$ -**2c**, and *ene*-products *ul*-**3c**, *lk*-**3c**.

SCHEME 3. Chemical Correlation for the Configurational Assignment of the Dioxetane



SCHEME 4. Stereoselective Photooxidative Cleavage of Oxazolidinone-Functionalized *E/Z* Encarbamates **1g**–**1k** with Phenethyl Substitution at the C-3' Position (50:50 Mixture of *R/S* Epimers at the C-3' Position) for the Formation of the MDB Product



with essentially perfect stereoselectivity for the encarbamates *Z*-**1b** to *Z*-**1e** and that it is independent of the R^1 substituent. The dioxetanes derived from *E*-**1b** to *E*-**1e** were too labile and cleaved readily at room temperature (Scheme 4), but the dioxetane **2** derived from *E*-**1i** was sufficiently stable to establish its absolute configuration by the chemical correlation of Scheme 3.

The exclusive chemoselectivity in favor of the [2 + 2]-cycloaddition for the phenethyl-substituted *E/Z* encarbamates (Table 1, entries 12–19) provides an ideal platform for a thorough investigation of the factors that control the stereoselection that leads to dioxetane **2** as a function of the stereogenic centers at the C-4 and C-3' positions and the *E/Z* geometry. Examination of Table 1 reveals the remarkable result that the stereoselectivity in the formation of the dioxetanes **2g**–**2k** with phenethyl-substitution is independent of both the configuration at the C-3' position (entries 12–19) and the size of

the R^1 substituent (Me, i Pr, Ph) at the C-4 position. For example, the *R*-configured (at the C-4 position) *Z* encarbamate affords the $1'S,2'S$ -**2** dioxetane (Figure 1) with complete stereocontrol, irrespective of the C-3' configuration (Table 1, entries 14 and 15). By employing the optical antipode at the C-4 position (*S* configuration), the expected $1'R,2'R$ -**2** dioxetane is obtained, which demonstrates that the stereochemical course of the photooxygenation is well-behaved (Table 1, entry 15).

For mechanistic guidance to assess the stereochemical course of the 1O_2 attack (see also section 4.4), we examined the X-ray structure of the *E/Z* encarbamates⁸ as well as the chemical correlation in Scheme 3. Based on the X-ray structure, the attack of 1O_2 on the double bond of the phenethyl-substituted *Z*-encarbamate, as shown in Figure 3, is evidently dictated by the C-4 substituent. In contrast, the approach of 1O_2 for the corresponding *E* isomer is likely aided by the established directing effect of the polar carbonyl group (Figure 2).¹⁴ Thus, the determining features for the stereocontrol in the *E*-encarbamate may be satisfactorily accounted for with conventional concepts.

There is, however, still a puzzling feature of the 1O_2 reaction with the *Z* encarbamates: if stereocontrol is determined by the C-4 substituent (R^1 = Me, i Pr, t Bu), one would expect a gradual increase in the stereoselectivity for the dioxetane **2** with increasing steric bulk of the R^1 substituent. Nevertheless,

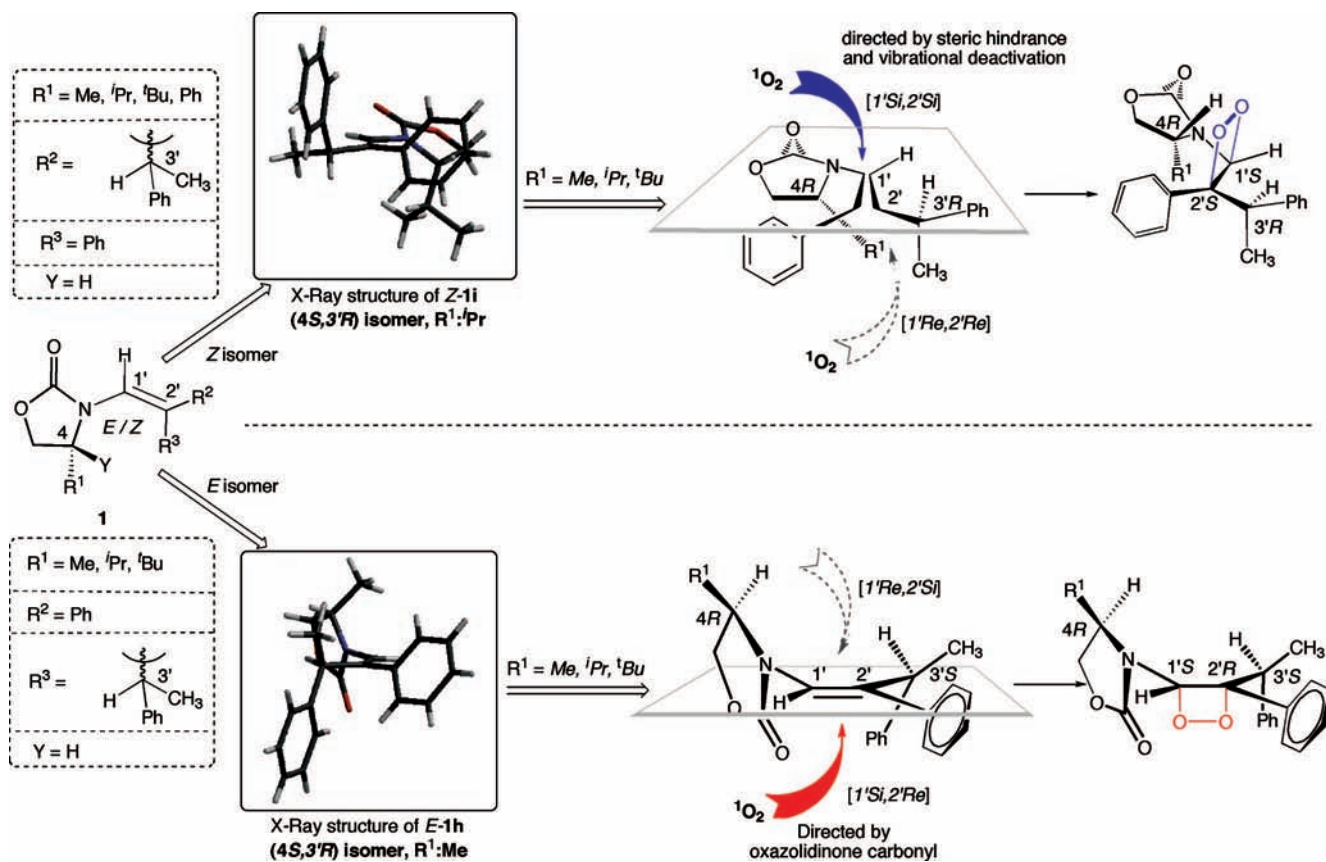


FIGURE 2. Preferred π -facial attack of $^1\text{O}_2$ in *Z*- (top) and *E*-enecarbamates (bottom). The conformations of the *E/Z*-enecarbamates are based on the X-ray structures of **Z-1i** and **E-1h**.

$$s = \frac{k_R}{k_S} = \frac{\ln[1 - C(1 + ee_{\text{MDB}})]}{\ln[1 - C(1 - ee_{\text{MDB}})]} \quad (1)$$

where C is the conversion and ee_{MDB} the ee value of the MDB

$$\ln(k_R/k_S) = \ln[(100 + \% ee_{\text{MDB}})/(100 - \% ee_{\text{MDB}})] \quad (2)$$

$$\ln(k_R/k_S) = \frac{\Delta\Delta S^\ddagger}{R} - \frac{\Delta\Delta H^\ddagger}{RT} \quad (3)$$

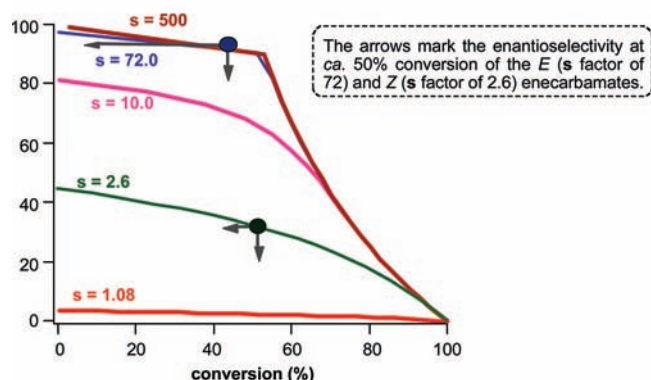


FIGURE 3. Enantiomeric excess (% ee) of the methyldeoxybenzoin (MDB) product versus conversion (%) for selected s factors plotted through eq 2.

the observed stereoselectivity (Table 1, entries 13–15 and 17) clearly contrasts with this expectation, which suggests that in

addition to steric effects, some unexpected factor appears to play a decisive role in controlling the extent of stereoselection in the dioxetane formation. We shall deal with this mechanistic puzzle in section 5.

3.3. Effect of the C-3' Substituents on the Diastereoselectivity of Dioxetane Formation.

With the stereoselectivity of dioxetane formation essentially perfect in regard to the C-4 substituent (Figure 1) for both *E/Z* configurations, now the effect of the C-3' substituent will be addressed, by assessing the enantiomeric excess (% ee) of the dioxetane cleavage product MDB (Scheme 4). The incentive was to test the efficacy of kinetic resolution (relative reactivity) of the epimeric enecarbamates **1** in their reaction with $^1\text{O}_2$. To determine how the stereoselectivity of the [2 + 2]-cycloaddition is affected by the configuration at the C-3' position, a 50:50 mixture of the *R/S*-phenethyl epimers was employed as a stereochemical reporter with fixed configuration (*R* or *S*) chosen for the C-4 position. For example, for **Z-1i** with the *i*Pr group at the *R*-configured C-4 position and a 50/50 mixture of *R/S*-configured phenethyl substituent at the C-3' position, kinetic resolution will favor the C-3'*S* epimer, because the C-3'*R* epimer reacted faster with $^1\text{O}_2$. Thus the stereoselectivity is rapidly

TABLE 2. Temperature and Solvent Effects on the Stereoselectivity Factor, s ,^a for the Formation of *R/S*-MDB Product in the Photooxygenation^b of Phenethyl-Substituted^c *Z*- and *E*-Encarbamates **1i**^d

entry	temp (°C)	CD ₂ Cl ₂ ^{ef} % ee; % convn; s			CDCl ₃ ^e % ee; % convn; s			CD ₃ CN ^{eo} ee; % convn; s	CD ₃ OD ^{eo} ee; % convn; s
		<i>Z/R</i>	<i>E/R</i>	<i>E/S</i>	<i>Z/R</i>	<i>Z/S</i>	<i>E/R</i>	<i>E/R</i>	<i>E/R</i>
1	50						8(<i>S</i>); 5; 1.2	64(<i>S</i>); 23; 5.5	70(<i>R</i>); 30; 7.6
2	18/20	22(<i>R</i>); 29; 1.7	34(<i>S</i>); 25; 2.3	28(<i>R</i>); 29; 2.0	28(<i>R</i>); 47; 2.2	26(<i>S</i>); 49; 2.1	63(<i>R</i>); 17; 5.0	30(<i>S</i>); 34; 2.1	85(<i>R</i>); 34; 19
3	-15/-20	22(<i>R</i>); 59; 2.1	27(<i>R</i>); 65; 2.7	36(<i>S</i>); 59; 3.4			78(<i>R</i>); 37; 13	0; 28; 1.0	90(<i>R</i>); 17; 23
4	-40	30(<i>R</i>); 56; 2.6	82(<i>R</i>); 54; 40	88(<i>S</i>); 56; 45			88(<i>R</i>); 43; 31	58(<i>R</i>); 37; 5.2	94(<i>R</i>); 12; 37
5	-70								97(<i>R</i>); 8; 72

^a Calculated from the % ee and % conversion data according to eqs 1–3. ^b Methylene blue was employed as sensitizer. ^c 50/50 mixture of the *R/S* epimers at the C-3' position in the Ph(Me)CH side chain was employed in this kinetic resolution. ^d *Z* and *E* diastereomers of **1i** were used with *R* or *S* configuration at the C-4 position in the oxazolidinone chiral auxiliary. ^e The % ee values and s factors were an average of at least 3 runs; error within 5% of the stated values. ^f For CD₂Cl₂, the temperature was +20 and -20 °C.

and quantitatively determined by measuring the ee values in the MDB product by GC analysis on a chiral stationary phase (Scheme 4).

4. Photooxidative Cleavage of the Encarbamates as a Stereoselectivity Probe of the C-3' Chirality in the Alkenyl Side Chain

Stereocontrol of the photooxidative cleavage of *E/Z*-encarbamates by ¹O₂ to the *R/S*-MDB product (Scheme 4) was studied in a range of solvents and at various temperatures (Table 2). Because the size of R¹ substituent at the C-4 position does not influence the extent of stereoselectivity in the photooxygenation, we shall take the isopropyl derivative **1i** as an exemplar. Table 2 clearly shows that the photooxygenation of the *E*-encarbamates yields significantly higher ee values for the MDB product (Scheme 4) than the corresponding *Z* isomers. For *E*-**1i** (*R* configuration at C-4 position) in CDCl₃ (Table 2, entry 2), the ee value of *R*-MDB for the *Z*-**1i** is 28%, whereas for the *E*-**1i**, it is 63%; thus, the *E* isomer displays over twice the stereoselectivity of the corresponding *Z* isomer. Evidently, by the simple choice of the *E/Z* geometry, the enantioselectivity may be more than doubled, highlighting the importance of the alkene geometry (*Z/E*). Further, the sense (*R* versus *S*) of the MDB product during photooxygenation of both *E/Z*-encarbamates depends on the configuration at the C-4 position. As expected, a change of the configuration at the C-4 position selects the opposite MDB enantiomer as the major product, indicating that the system is well-behaved.

A pertinent feature still to be analyzed concerns the role of the C-3' configuration in the phenethyl substituent on the stereoselectivity. In view of kinetic resolution, the ee values of the MBD product do not suffice for quantification of the stereocontrol, since they depend on the extent of conversion. For this reason, we have chosen the *stereoselectivity factor*, s ,^{15,16} (section 4.1), as a convenient quantitative parameter for the

mechanistic analysis of the stereochemical effects imposed by the C-3' configuration in the phenethyl substituent.

4.1. The Stereoselectivity Factor (s) for the Mechanistic Diagnosis of the Stereochemical Course in the Photooxidative Cleavage of the Encarbamates as a Function of the C-3' (*R/S*) Chirality. The stereoselectivity factor s ,^{15,16} as defined by eq 1 (Figure 3), is the ratio of rates of formation (rate constants) for the *R*- and *S*-MDB product. Further, the s factor represents the ee values corrected for the extent of conversion (efficiency of the kinetic resolution). Figure 3 (plot of % ee versus % convn) illustrates the fundamental difference between the s factor and the ee value,^{15,16} in which the dependence of the enantioselectivity on conversion for selected s factors of 1.08, 2.6, 10.0, 72.0, and 500 are displayed, computed for a hypothetical case according to eq 2 (Figure 3). A high value of the s factor (>70) corresponds to a high ee value (>97%) in the MDB product even at ~50% conversion, while an s factor of only ~3 implies a relatively low ee value (~30%) at ~50% conversion.

The similar s factors for the photooxidative cleavage of the *E*-encarbamates with differently sized R¹ substituents at the C-4 position demonstrate the insensitivity of ¹O₂ toward steric bulk in this reaction. For example, in CDCl₃ at +18 °C the s factors are 5.9 for *E*-**1h** (methyl) and 5.0 for *E*-**1i** (isopropyl) derivatives, which convincingly illustrate the lack of response of the stereoselectivity toward the size variation of the R¹ substituent. Since the size of R¹ substituent at the C-4 position does not affect the extent of the stereoselection in the photooxygenation process, we will limit our subsequent discussion to the isopropyl-substituted *Z/E*-encarbamates **1i**.

4.2. Mechanistically Intriguing Solvent and Temperature Effects in the Photooxidative Cleavage of the *E/Z* Encarbamates by ¹O₂ as a Function of the C-3' (*R/S*) Chirality. From Table 2, it is clear that the stereoselectivity for the photooxidative cleavage of the *Z*-encarbamates is relatively insensitive to solvent and temperature variations

(entries 2–4 for CD_2Cl_2 and entry 2 for CDCl_3 for $Z/R\text{-1i}$), whereas for the E -enecarbamates it is extremely sensitive (entries 2–4 for CD_2Cl_2 , CDCl_3 , and CD_3CN and entries 1–5 for CD_3OD for $E/R\text{-1i}$). We shall examine the response of the s factor to the imposed solvent and temperature variations to understand the mechanistically intriguing dichotomy in the stereoselectivity exhibited by the E/Z -enecarbamates. The configurational sense of the MDB product switches with the change in the configuration (R or S) at C-4 position as expected with similar % ee values (within the experimental error), as exemplified for the $E\text{-1i}$ (C-4R) and $E\text{-1i}$ (C-4S) in CD_2Cl_2 (Table 2, entries 2–4) at the different temperatures.

The effect of the solvent polarity was examined by selecting the polar aprotic CD_3CN , the polar protic CD_3OD , and the relatively low-polar halogenated solvents CD_2Cl_2 and CDCl_3 . For the photooxidative cleavage of the $E\text{-1i}$ C-4R substrate, the solvent dependence of the stereoselectivity (% ee) follows the order CD_3CN (30%) \approx CD_2Cl_2 (34%) $<$ CDCl_3 (63%) $<$ CD_3OD (85%) at 18–20 °C (Table 2, entry 2 for $E/R\text{-1i}$ in CD_3CN , CD_2Cl_2 , CDCl_3 , CD_3OD). The finding that the R -MDB enantiomer is the favored product in CDCl_3 and CD_3OD but the S -MDB dominates in CD_2Cl_2 and CD_3CN reveals that the stereoselectivity cannot be attributed to the solvent polarity alone.

Still more mechanistically intriguing is the temperature dependence of the ee values for the $E\text{-1i}$ substrate, as well as the enhanced stereoisomer of the MDB product. In CD_3OD , the extent of the stereoselectivity is relatively constant over a broad temperature range from –70 to +50 °C with the same enantiomer (R -MDB) being formed (Table 2, entries 1–5). In the other solvents, depending on the temperature, a change in the configurational sense of the MBD product is observed. For example, as shown in Table 2, very good stereocontrol in favor of the R -MDB is found in chloroform- d at –40 °C (88% ee, $s = 31$, entry 4), but the S -MDB is preferred in very poor stereoselectivity at +50 °C (8% ee, $s = 1.2$, entry 1). The inflection in the enantioselectivity sense (R to S) occurs in CDCl_3 above +18 °C, in CD_2Cl_2 between –20 and +20 °C (entries 1 and 2 for CDCl_3 and entries 2–3 for CD_2Cl_2), and in CD_3CN at –15 °C (entry 3). These remarkable solvent and temperature effects forebode complex mechanistic behavior.

4.3. A Photo-Pasteur Kinetic Resolution of the MDB Enantiomers with Singlet Oxygen. One of the striking results shown in Table 2 is the very high stereocontrol (>97%; nearly perfect stereocontrol!) observed in CD_3OD at –70 °C for the E -enecarbamate, which allows for the nearly complete

separation of the R/S -MDB enantiomers. Photooxygenation of a 50/50 mixture of the R/S -epimers (C-3' phenethyl substituent) of the C-4R-configured $E\text{-1i}$ substrate in CD_3OD at –70 °C was carried out close to 50% conversion (essentially complete consumption of the C-3'R-configured $E\text{-1i}$) to afford the R -MDB product almost exclusively (Figure 4). The MDB product was separated from the photooxygenate by chromatography, and the remaining C-3'S-configured C-4R- $E\text{-1i}$ epimer was quantitatively photooxidized at room temperature to give the S -MDB product with an ee value of 97%. We coin this photooxidative kinetic resolution of the MDB optical isomers as a *photochemical Pasteur*-type experiment. To highlight the importance of s factor in this kinetic resolution, the photooxygenations of the E isomer ($s = 72$, CD_3OD) versus the Z isomer ($s = 2.6$, CD_2Cl_2) of the enecarbamates are contrasted in Figure 4. At best, only 30% ee may be achieved for the Z isomer, whereas for the E isomer the kinetic resolution is nearly perfect. This stereochemical dichotomy between the E/Z -enecarbamates demands a mechanistic explanation.

4.4. Mechanistic Rationale of the Stereoselectivity as a Function of the C-3' Chirality in the Photooxygenation of Enecarbamates. The conspicuously complex temperature and solvent effects shall now be mechanistically scrutinized to understand the stereoselectivity during photooxidative cleavage of the E/Z -enecarbamates. Temperature and solvent variations, as observed in Table 2, are well-known for systems for which there are enthalpy–entropy compensations.^{17–19} Thus, to determine whether a compensation effect provides a mechanistic understanding of the temperature dependence of the ee values for the MDB product, we shall examine the differential activation parameters ($\Delta\Delta S^\ddagger$, $\Delta\Delta H^\ddagger$) for the photooxygenation of E/Z -enecarbamates in various solvents. The parameters for the photooxygenation of $E\text{-1i}$ and $Z\text{-1i}$ enecarbamates were computed by using the Eyring relation (eq 3). The ee values showed a pronounced temperature dependence (Table 2) in CDCl_3 , CD_2Cl_2 , and CD_3CN for the $E\text{-1i}$ enecarbamate, corroborated by a relatively high contribution by the entropy term ($|\Delta\Delta S^\ddagger| \geq 14$ cal/(mol K)) and an appreciable contribution by the enthalpy term ($|\Delta\Delta H^\ddagger| \approx 4$ kcal/K).²⁰

The change in the % ee values (or $\Delta\Delta G^\ddagger$) depends on both the entropic and enthalpic terms. Since the $\Delta\Delta H^\ddagger - S^\ddagger/(RT)$ term is proportional to the reciprocal temperature (eq 3), the $\ln(k_R/k_S)$ value is determined mostly by the enthalpic contribution at low temperatures; however, as the temperature increases, the relative contribution from the $\Delta\Delta S^\ddagger - S^\ddagger/R$ term increases and begins to override the $\Delta\Delta H^\ddagger - S^\ddagger/(RT)$ term at some characteristic temperature. Eventually, the sign of the $\ln(k_R/k_S)$

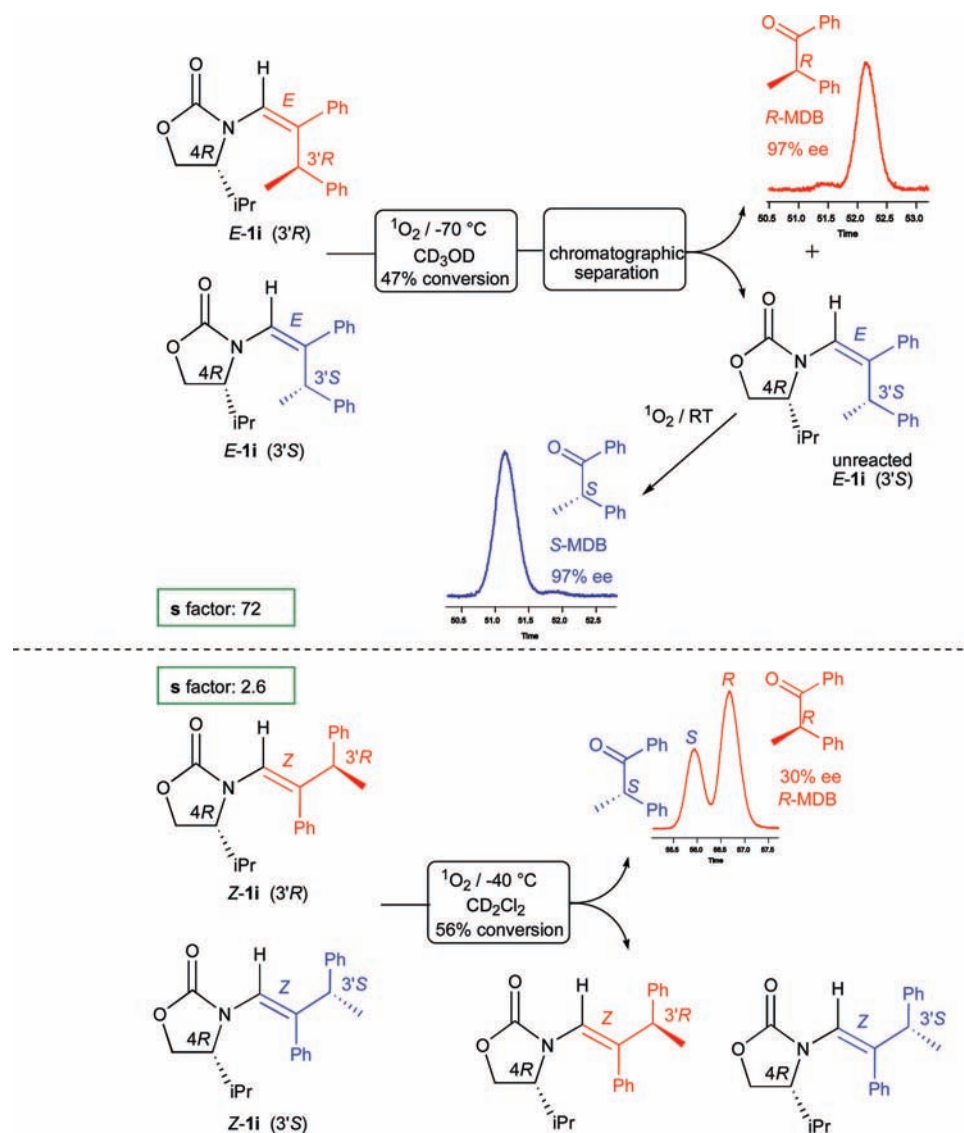


FIGURE 4. Photochemical kinetic resolution of MDB (photochemical Pasteur-type experiment) in the photooxygenation of *E*-1*i* (top) and *Z*-1*i* (bottom).

value inverts, and the configurational sense in the enantioselectivity switches, provided that the $\Delta\Delta H^{\ddagger}$ and $\Delta\Delta S^{\ddagger}$ terms possess the same sign, as is the case here for the photooxygenation of the *E* isomer (Table 2). Such entropy effects may be associated with temperature- and solvent-dependent conformational factors, which in the present case are presumably dictated by the stereogenic center at the C-3' phenethyl substituent.

In contrast, the corresponding relative insensitivity of *Z*-1*i* enecarbamates to temperature and solvent variation is convincingly explained by the near-zero $\Delta\Delta S^{\ddagger}$ and $\Delta\Delta H^{\ddagger}$ terms in CD_2Cl_2 .²⁰ Most importantly, the signs of $\Delta\Delta S^{\ddagger}$ and $\Delta\Delta H^{\ddagger}$ are opposite. Consequently, their contributions compensate each other on temperature variation, which results in comparable ee values for the *Z*-enecarbamates (Table 2).

Similarly, for *E*-1*i* in the protic CD_3OD , the observed small temperature dependence is again corroborated by the low $\Delta\Delta S^{\ddagger}$ and $\Delta\Delta H^{\ddagger}$ values (but both have the same sign).²⁰ Consequently, the contribution from $\Delta\Delta H^{\ddagger}$ will increase only slightly upon decreasing the temperature, which corresponds to a small response in the stereoselectivity; also the sense of the enantioselectivity is not changed.²⁰ Moreover, the enthalpy–entropy plot for both *E*- and *Z*-enecarbamates²⁰ shows that the differential activation parameters fall on a single straight line that passes through the origin, which indicates that the same diastereo-differentiating mechanism operates, irrespective of (a) the configuration of the alkene [*E*/*Z*], (b) the R^1 substituent at the C-4 position [Me, *i*Pr, *t*Bu], (c) the configuration [*R*/*S*] at the C-4 position, and (d) the employed solvent.

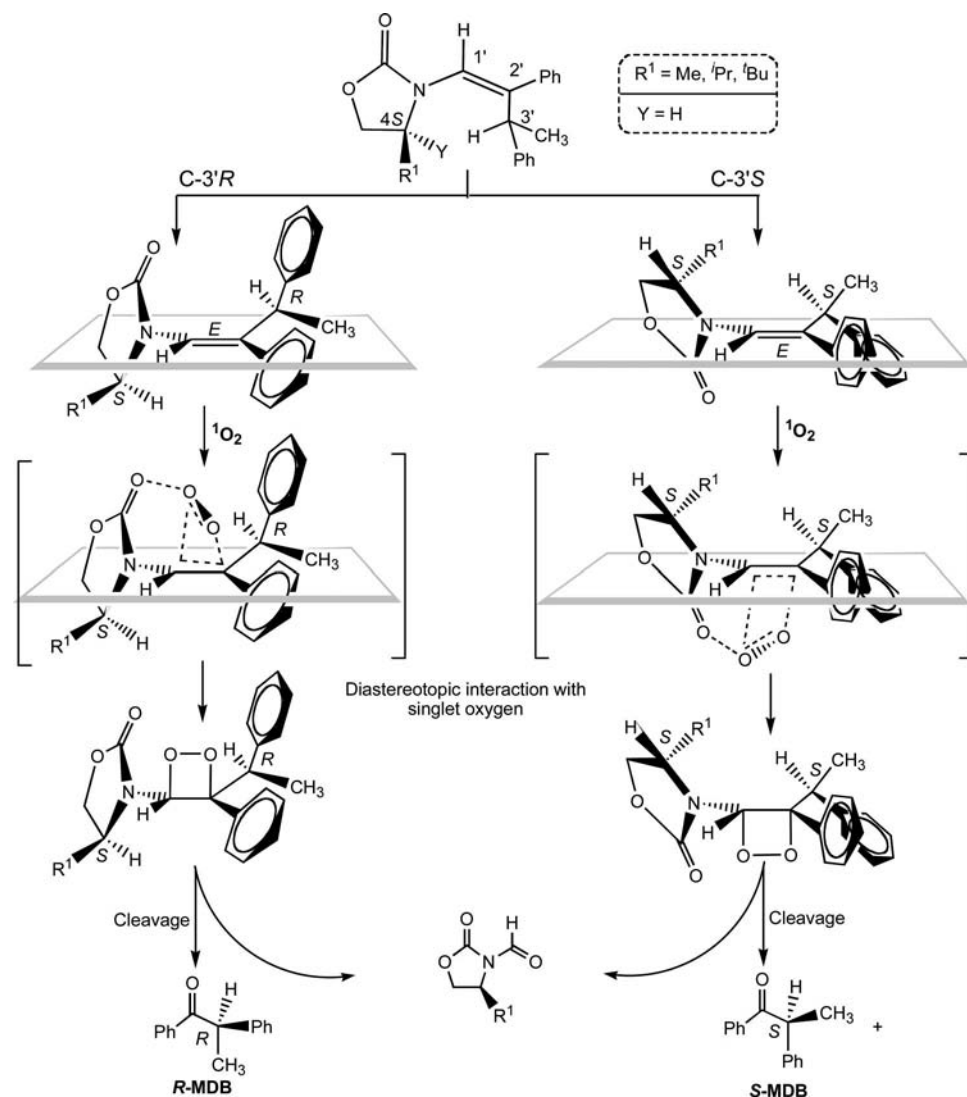


FIGURE 5. Preferred conformational alignment of the oxazolidinone ring and the phenethyl substituent in epimeric *E*-enecarbamates and the expected stereoselective attack by $^1\text{O}_2$. Note that the orientation of the oxazolidinone carbonyl group depends on the chirality of the C-3' position. The structure is based on the X-ray analysis or the *R* and *S* C-3' epimers of *E*-**1h** with *S* configuration at the C-4 position. The C-4 substituent of the oxazolidinone is not expected to alter the relative orientations of oxazolidinone carbonyl group, the alkene double bond, and the C-3' phenethyl group.

Detailed mechanistic rationalization on the favored stereochemical trajectory of $^1\text{O}_2$ attack^{8,20} on the C=C of the *E/Z*-enecarbamate was provided by X-ray crystallography, as we succeeded in assessing the structural details of the crystalline methyl-substituted *E*-**1h** and the isopropyl-substituted *Z*-**1i** derivatives. The conformations inferred from the X-ray structures of *E*-**1h** and *Z*-**1i** serve as a first-order approximation for the $^1\text{O}_2$ attack on the enecarbamates, as revealed in Figure 5.

Figure 5 illustrates the nonplanar orientation of the oxazolidinone carbonyl group in the *E* isomer in contrast to the coplanar alignment in the *Z* isomer (Figure 2). Inspection of the crystal structure of both *E*-enecarbamate epimers (*R* configurations at the C-4 and *R/S* at the C-3' positions) reveals that the oxazolidinone carbonyl group is almost perpendicular to

the plane of the double bond. Further, the C-3' configuration dictates the orientation of the oxazolidinone carbonyl group in the *E*-enecarbamate (Figure 5; in C-4*R* *E*-**1i**, the carbonyl group is below the plane of the double bond for the C-3'*S* but above for the C-3'*R* epimer), whereas for the *Z*-enecarbamate the orientation of the oxazolidinone ring is unaffected by the C-3' configuration.

We speculate that the *E* isomers are more flexible than the corresponding *Z* isomers due to steric encumbrance between the imposing phenyl ring of the phenethyl-substituent and the C-4 substituent, which reflect the difference in the diastereomeric interactions between the C-3'*R* and C-3'*S* epimers, as illustrated in Figure 5. Therefore, the *E*-enecarbamates are susceptible to solvent and temperature variations, as corrobo-

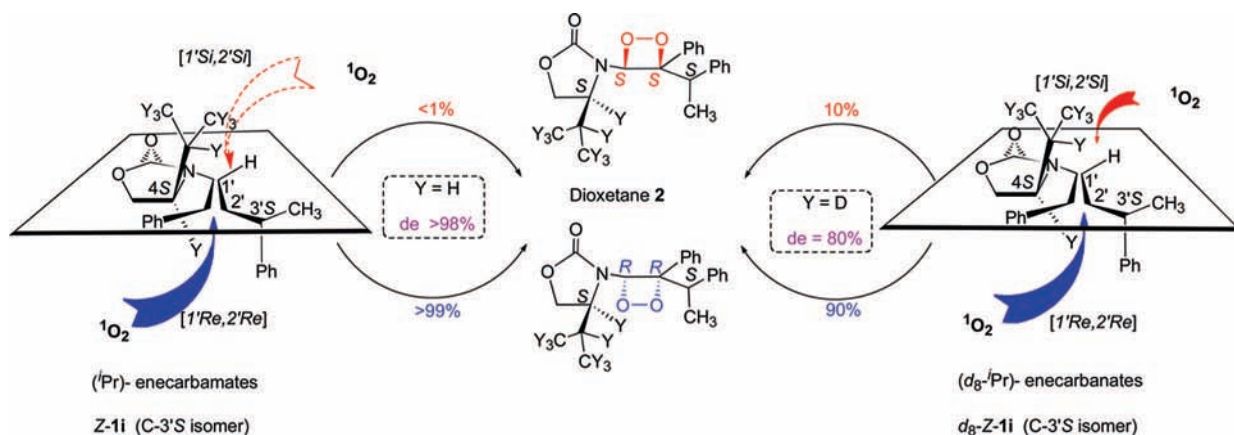


FIGURE 6. Steric interactions and vibrational quenching in the stereoselective π -facial attack of $^1\text{O}_2$ for deuterated (d_8 -**Z-1i**) versus undeuterated (**Z-1i**) enecarbamates.

rated by the $\Delta\Delta S^\ddagger$ and $\Delta\Delta H^\ddagger$ values. Nonetheless, although it is well-known that polar groups may facilitate the facial selectivity of $^1\text{O}_2$,¹⁴ in the present case close to equal amounts of the *R/S*-MDB enantiomers would be expected as products, since the relative spatial arrangement of the carbonyl and the phenethyl groups are very similar in both structures. Clearly, the very high stereoselectivity for the *E* isomer implies that other physical interactions between the oxidant and substrate must be involved, which presumably relate to the electronically excited reactant.

5. Excited-State Deactivation of Singlet Oxygen as Mode of Stereoselectivity Control

It seems truly remarkable that the smallest possible oxidant, $^1\text{O}_2$, is subject to such high stereocontrol in the present [2 + 2]-cycloaddition reaction. Indeed, moderate stereoselectivity was observed for O_3 , an oxidant comparable in size to $^1\text{O}_2$,^{12,21} with negligible solvent and temperature effects. Evidently, for the electronically excited oxidant ($^1\text{O}_2$), stereocontrol is promoted by some factor in addition to the usual steric interaction between the substrate and reactant. Since for $^1\text{O}_2$ its chemical reaction competes with its physical deactivation to unreactive $^3\text{O}_2$,^{5–7,22} we speculate that during the $^1\text{O}_2$ attack, superimposed on the usual steric interactions, one stereochemical pathway is physically deactivated more rapidly, which results in enhanced stereoselectivity. For example, the high stereocontrol in the dioxetane formation (Table 1) is the consequence of both steric effects in the chemical reactivity (Section 3) and selective π -facial quenching of the $^1\text{O}_2$ by vibrational deactivation. In this context, it is well-known that the lifetime of $^1\text{O}_2$ in deuterated solvents is longer than that in nondeuterated ones, since C–H bond vibrations deactivate $^1\text{O}_2$ to its triplet ground state.^{5–7,22} Consequently, to test

TABLE 3. The Effects of Steric Interaction and Vibrational Quenching on the Diastereoselectivity in the Alkylation and Photooxygenation of Substrates with Oxazolidinone Chiral Auxiliaries

R ¹	Diastereoselectivity (% de)	
	Alkylation ^a	photooxygenation ^b
Me	72	> 98
ⁱ Pr	81	> 98
^t Bu	> 98	> 98

^a Alkylation of enolates (values taken from ref 23). ^b Photooxygenation of enecarbamates ($\pm 5\%$ error of stated value); optically pure at the C-4 and C-3' positions.

experimentally the conjecture of stereoselective vibrational deactivation of $^1\text{O}_2$, we compared the stereoselectivity in the dioxetane formation of the deuterated d_8 -**Z-1i** with the undeuterated **Z-1i** substrate. Indeed, the photooxygenation of d_8 -**Z-1i** displayed only 80% stereoselectivity compared with >98% for undeuterated **Z-1i** (Figure 6). We attribute the substantial difference in the stereoselectivity between d_8 -**Z-1i** and **Z-1i** to the *stereoselective vibrational deactivation* of $^1\text{O}_2$ by the C–H bonds in the $\text{CH}(\text{CH}_3)_2$ substituent, compared with the C–D bonds in the $\text{CD}(\text{CD}_3)_2$ group. The stereoselectivity in the deuterated d_8 -**Z-1i** is similar in magnitude ($\sim 80\%$ for ⁱPr) to that reported for the enolate alkylation of oxazolidinone derivatives, for which only steric effects apply (Table 3).²³ Thus, the stereocontrol in the undeuterated **Z-1i** substrate displays the composite effects of the classical steric interactions ($\sim 80\%$ contribution) and the novel vibrational deactivation ($\sim 20\%$ contribution).

To substantiate further the role of excited-state deactivation in the photooxygenation of the *E/Z*-enecarbamates, the

rate constants for the chemical reaction and physical quenching were determined by competitive kinetics.^{20,24} Under similar conditions, the ratio of rate constants ($k_R/k_S = 1.3$; +18 °C) for the C-3'R to C-3'S epimers with a fixed C-4 configuration is in reasonable agreement with the *s* factor ($k_R/k_S = 2.1$; +20 °C) data in Table 2. A significant result of these kinetic studies is the fact that the chemical reaction is about an order of magnitude slower than the physical quenching,²⁰ which enables the excited oxidant to sense the effect of the vibrational interaction on the stereoselectivity. For emphasis, *if the rate of the chemical reaction is too fast and higher than that of the physical quenching, the role of vibrational deactivation will be insignificant and, thus, go undetected.*

5.1. A New Paradigm in Controlling the Stereoselectivity in Photochemical Reactions. The present photooxygenation of enecarbamates conspicuously demonstrates that stereoselectivity and presumably other types of selectivities are subject not only to the traditional steric control that governs ground-state reactions but also to selective physical deactivation of the electronically excited reactant. In our model system, the vibrational deactivation of $^1\text{O}_2$ by C–H bonds operates in concert with the classical steric interactions to achieve essentially perfect stereocontrol in the photooxidative cleavage of the enecarbamates. In principle, one may envisage similar excited-state deactivation as an effective mode to manipulate selectivity generally in photoreactions, provided the chemical reactivity proceeds at a lower rate than physical deactivation. If this premise is valid, a stereogenic center in the proximity of the reaction site may physically deactivate the incoming electronically excited reactant from one face more effectively than from the other, and significant stereoselectivity should ensue. Hence, for a photochemical reaction, unlike for ground-state reactions, in addition to steric encumbrance (Cram, Karabatsos, and Felkin–Ahn models), excited-state deactivation also applies.

As illustrated in Figure 7, in a ground-state reaction, steric interactions dictate the preferential attack of the incoming reactant on the prochiral face of the reaction site (Figure 7, left). In photoreactions, however, physical deactivation of the excited state (Figure 7, right), in concert with the steric interactions, may determine the selectivity. For example, as illustrated for the present case in Figure 7, the steric interaction on the attacking $^1\text{O}_2$ is about the same, but its vibrational deactivation is significantly stronger by the CH_3 than by the CD_3 group; thus, enhanced stereoselection results over and beyond the usual steric factors within the substrate. We surmise that physical deactivation of excited states could be fine-tuned to play a significant role in stereoselectivity.

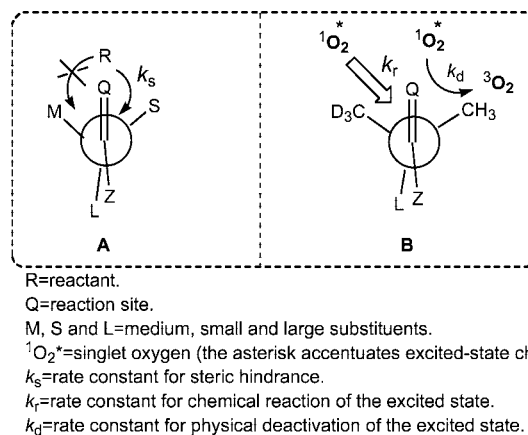


FIGURE 7. Stereoselectivity control imposed by steric hindrance (A, ground-state reactivity) and by physical deactivation (B, excited-state reactivity) in the photooxygenation of enecarbamates.

6. Conclusion

In this Account, we have tried to impress upon the reader that the extensive stereochemical properties embodied in the chiral enecarbamates make these substrates informative molecular probes to diagnose stereochemical control in photoreactions. Through the appropriate choice of substituents in the enecarbamate, the mode selectivity (*ene* versus [2 + 2]), which depends on the alkene geometry, the steric bulk of the C-4 oxazolidinone-substituent, and the C-3' configuration, may be manipulated. By employment of a C-3' phenethyl substituent as a stereochemical reporter, [2 + 2] mode takes place exclusively to afford dioxetane in high stereoselectivity. Such a high degree of stereoselection in the photooxygenation enabled the isolation of the optically pure MDB enantiomers (after dioxetane decomposition) by means of a photochemical-Pasteur-type separation. The high stereoselectivity in the dioxetane formation is rationalized in terms of the established *steric hindrance*, in concert with the unprecedented *vibrational deactivation* of the incoming electronically excited $^1\text{O}_2$. Future efforts should be expended to generalize this novel phenomenon for other photochemical transformations.

We dedicate this Account to Professor F. D. Greene, an esteemed scientist and appreciated friend, on the occasion of his 80th birthday. The authors at Columbia thank the NSF (Grant CHE-04-15516) for generous support of this research. W.A. is grateful for the financial support from the Deutsche Forschungsgemeinschaft, Alexander-von-Humboldt Stiftung, and the Fonds der Chemischen Industrie. S.J. thanks NDSU for financial support through a faculty start-up grant. T.P. acknowledges the support of the W.M. Keck Foundation.

Supporting Information Available. The differential activation parameters, Eyring plot, X-ray structures of *E/Z*-enecarbamates, table of differential activation parameters for photooxygenation, and the rate constant for total quenching and chemical reaction for photooxygenation. This material is available free of charge via the Internet at <http://pubs.acs.org>.

BIOGRAPHICAL INFORMATION

J. Sivaguru is currently an Assistant Professor at the Department of Chemistry and Molecular Biology, North Dakota State University. He earned his B.Sc. at St. Joseph's College, Trichy, and M.Sc. at Indian Institute of Technology, Chennai, India, following which he came to the United States of America for his Ph.D., to work in the laboratory of Prof. V. Ramamurthy. Upon obtaining his Ph.D. degree (2003) at Tulane University, he moved to Columbia University as a Postdoctoral Fellow to work under the direction of Prof. Nicholas J. Turro (2003–2006). His current research effort at NDSU focuses on photochemical reactions in nanocavities and constrained environments, host–guest chemistry, molecular recognition in chemical and biological systems, and asymmetric photoreactions in solution.

Marissa Solomon is a graduate student with Prof. Turro's group at Columbia University. Her research focus has been solution and supramolecular photochemistry utilizing singlet oxygen and ozone, as well as luminescent probes for biological applications.

Thomas Poon received his B.S. in chemistry from Fairfield University and his Ph.D. in chemistry at UCLA under the direction of Christopher S. Foote. Poon was a Camille and Henry Dreyfus Postdoctoral Fellow under Bradford P. Mundy at Colby College. He began his academic career at Randolph-Macon College in Virginia and is currently Associate Professor of Chemistry at the Claremont McKenna, Pitzer, and Scripps Colleges in Claremont, California.

Steffen Jockusch received his Ph.D. degree in 1993 from the Martin Luther University Halle-Wittenberg in Merseburg (Germany) with Prof. H.-J. Timpe. In 1994, he joined Prof. Turro's research group at Columbia University as a postdoctoral fellow, and since 1997, he has been an associate research scientist. His research interests include spectroscopic investigations of reactive intermediates in photophysical and photochemical processes, supramolecular photochemistry, and luminescent probes for biological applications.

Sara G. Bosio received her Ph.D. degree in 2003 at the University of Würzburg, Germany, with Prof. Adam. Currently, she is employed at Phenex Pharmaceuticals AG, Germany.

Waldemar Adam, born in 1937 in Alexanderdorf, Ukraine, received his B.Sc. degree from the University of Illinois (1958) and Ph.D. degree from MIT (1961, F. D. Greene). He was appointed Assistant Professor (1961) and promoted to Full Professor (1970) by the University of Puerto Rico (Rio Piedras). In April 1980, he was assigned the Chair of Organic Chemistry at

the University of Würzburg (Germany) and was retired in October 2002. In December 2006, he was awarded Professor Emeritus status by the University of Puerto Rico. He has published over 995 papers on photochemistry, peroxides (dioxetanes, dioxiranes), radicals, and singlet oxygen, for which he earned numerous awards.

Nicholas J. Turro has been teaching at Columbia University since 1964 and is currently the Wm. P. Schweitzer Professor of Chemistry and Professor of Chemical Engineering and Applied Chemistry, as well as Professor of Earth and Environmental Engineering. He has written over 800 scientific publications and 2 textbooks on molecular photochemistry. His recent awards include the 2005 Theodor Förster Award from the German Chemical Society and the 2007 Nichols Medal by the New York Section of the American Chemical Society. He is a member of the National Academy of Sciences and the American Academy of Arts and Sciences.

FOOTNOTES

*To whom correspondence should be addressed. E-mail addresses: sivaguru.jayaraman@ndsu.edu; wadam@chemie.uni-wuerzburg.de; njt3@columbia.edu.

REFERENCES

- 1 Chiral Photochemistry, Inoue, Y., Ramamurthy, V.; Eds.; Marcel Dekker: New York, 2004.
- 2 Inoue, Y. Asymmetric photochemical reactions in solution. *Chem. Rev.* **1992**, *92*, 741–770.
- 3 Rau, H. Asymmetric photochemistry in solution. *Chem. Rev.* **1983**, *83*, 535–547.
- 4 Turro, N. J. Supramolecular organic photochemistry: control of covalent bond formation through noncovalent supramolecular interactions and magnetic effects. *Proc. Natl. Acad. Sci. U.S.A.* **2002**, *99*, 4805–4809.
- 5 *Singlet Oxygen*, Wasserman, H. H., Murray, R. W.; Eds.; Academic Press: New York, 1979.
- 6 *Singlet Oxygen*, Frimer, A. A.; Ed.; CRC Press: Boca Raton, FL, 1985; Vols. 1–4.
- 7 Foote, C. S. Photosensitized oxygenations and the role of singlet oxygen. *Acc. Chem. Res.* **1968**, *1*, 104–110.
- 8 Adam, W.; Bosio, S. G.; Turro, N. J.; Wolff, B. T. Enecarbamates as selective substrates in oxidations: Chiral-auxiliary-controlled mode selectivity and diastereoselectivity in the [2 + 2] cycloaddition and ene reaction of singlet oxygen and in the epoxidation by DMD and mCPBA. *J. Org. Chem.* **2004**, *69*, 1704–1715.
- 9 Sivaguru, J.; Poon, T.; Franz, R.; Jockusch, S.; Adam, W.; Turro, N. J. Stereoselective control within confined spaces: Enantioselective photooxidation of enecarbamates inside zeolite supercages. *J. Am. Chem. Soc.* **2004**, *126*, 10816–10817.
- 10 Sivaguru, J.; Saito, H.; Solomon, M. R.; Kaanumalle, L. S.; Poon, T.; Jockusch, S.; Adam, W.; Ramamurthy, V.; Inoue, Y.; Turro, N. J. Control of chirality by cations in confined spaces: Photooxidation of enecarbamates inside zeolite supercages. *Photochem. Photobiol.* **2006**, *82*, 123–131.
- 11 Poon, T.; Sivaguru, J.; Franz, R.; Jockusch, S.; Martinez, C.; Washington, I.; Adam, W.; Inoue, Y.; Turro, N. J. Temperature and solvent control of the stereoselectivity in the reactions of singlet oxygen with oxazolidinone-substituted enecarbamates. *J. Am. Chem. Soc.* **2004**, *126*, 10498–10499.
- 12 Sivaguru, J.; Poon, T.; Hooper, C.; Saito, H.; Solomon, M.; Jockusch, S.; Adam, W.; Inoue, Y.; Turro, N. J. A comparative mechanistic analysis of the stereoselectivity trends observed in the oxidation of chiral oxazolidinone-functionalized enecarbamates by singlet oxygen, ozone and triazolidinone. *Tetrahedron* **2006**, *62*, 10647–10659.
- 13 Sivaguru, J.; Solomon, M. R.; Saito, H.; Poon, T.; Jockusch, S.; Adam, W.; Inoue, Y.; Turro, N. J. Conformationally controlled (entropy effects), stereoselective vibrational quenching of singlet oxygen in the oxidative cleavage of oxazolidinone-functionalized enecarbamates through solvent and temperature variations. *Tetrahedron* **2006**, *62*, 6707–6717.
- 14 Prein, M.; Adam, W. The Schenck ene reaction: Diastereoselective oxyfunctionalization with singlet oxygen in synthetic applications. *Angew. Chem., Int. Ed. Engl.* **1996**, *35*, 471–494.

- 15 Kagan, H. B.; Fiaud, J. C. Kinetic resolution. *Top. Stereochem.* **1988**, *18*, 249–330.
- 16 Keith, J. M.; Larrow, J. F.; Jacobsen, E. N. Practical considerations in kinetic resolution reactions. *Adv. Synth. Catal.* **2001**, *343*, 5–26.
- 17 Leffler, J., E. The enthalpy–entropy relationship and its implications for organic chemistry. *J. Org. Chem.* **1955**, *20*, 1202–1231.
- 18 Leffler, J., E. The interpretation of enthalpy and entropy data. *J. Org. Chem.* **1966**, *31*, 533–537.
- 19 Buschmann, H.; Scharf, H.-D.; Hoffmann, N.; Esser, P. The isoinversion principle - a general model of chemical selectivity. *Angew. Chem., Int. Ed. Engl.* **1991**, *30*, 477–515.
- 20 Refer Supporting Information for details.
- 21 Sivaguru, J.; Saito, H.; Poon, T.; Omonuwa, T.; Franz, R.; Jockusch, S.; Hooper, C.; Inoue, Y.; Adam, W.; Turro, N. J. Stereoselective photooxidation of enecarbamates: Reactivity of ozone vs singlet oxygen. *Org. Lett.* **2005**, *7*, 2089–2092.
- 22 Turro, N. J. The role of intersystem crossing steps in singlet oxygen chemistry and photo-oxidations. *Tetrahedron* **1985**, *41*, 2089–2098.
- 23 Evans, D. A.; Chapman, K. T.; Hung, D. T.; Kawaguchi, A. T. Transition state π -solvation by aromatic rings: An electronic contribution to Diels-Alder reaction diastereoselectivity. *Angew. Chem., Int. Ed. Engl.* **1987**, *26*, 1184–1186.
- 24 Poon, T.; Turro, N. J.; Chapman, J.; Lakshminarasimhan, P.; Lei, X.; Jockusch, S.; Franz, R.; Washington, I.; Adam, W.; Bosio, S. G. Stereochemical features of the physical and chemical interactions of singlet oxygen with enecarbamates. *Org. Lett.* **2003**, *5*, 4951–4953.